

# Visualizing electron delocalization, electron-proton correlations, and the Einstein-Podolsky-Rosen paradox during the photodissociation of a diatomic molecule using two ultrashort laser pulses

Szczepan Chelkowski\* and André D. Bandrauk

*Laboratoire de Chimie Théorique, Faculté des Sciences, Université de Sherbrooke, Sherbrooke Qc, J1K 2R1 Canada*

(Received 12 February 2010; published 1 June 2010)

We investigate theoretically the dissociative ionization of an  $\text{H}_2^+$  molecule using two ultrashort laser (pump-probe) pulses. The pump pulse prepares a dissociating nuclear wave packet on an ungerade surface of  $\text{H}_2^+$ . Next, an ultraviolet [or extreme ultraviolet (XUV)] probe pulse ionizes this dissociating state at large ( $R = 20\text{--}100$  bohr) internuclear distance. We calculate the momenta distributions of protons and photoelectrons which show a (two-slit-like) interference structure. A general, simple interference formula is obtained which depends on the electron and protons momenta, as well as, on the pump-probe delay and also on the durations and polarizations of the laser pulses. This pump-probe scheme reveals a striking quantum delocalization of the electron over two protons which intuitively should be localized on just one of the protons separated by the distance  $R$  much larger than the atomic Bohr orbit.

DOI: [10.1103/PhysRevA.81.062101](https://doi.org/10.1103/PhysRevA.81.062101)

PACS number(s): 03.65.Ud, 82.53.Kp, 33.80.Gj, 33.80.Eh

## I. INTRODUCTION

Recently, due to the extraordinary increase of research activities in quantum information and quantum cryptography there is a growing interest in various quantum intriguing phenomena originating back to the famous Einstein-Podolsky-Rosen (EPR) paradox [1] formulated in 1935. This paradox is related to the phenomenon of quantum entanglement [3] and to the nonlocal character of quantum mechanics [5] or to the problem of local realism versus the completeness of quantum mechanism. A most recent comprehensive review of various aspects of the EPR paradox can be found in [2]. So far nearly all experimental evidence for entanglement is related to the measurement of correlated photon pairs obtained in a process called “parametric down-conversion” [4]. In such processes a photon from a laser beam gets absorbed by an atom which subsequently emits two “polarization-entangled” photons. The entanglement phenomenon should in principle also appear in various breakup processes involving slower (massive) fragments than photons (e.g., in various disintegration processes such as photoionization and photodissociation), as suggested in [6–11]. So far, there exist very few experimental results demonstrating the entanglement in such slower processes and involving massive particles which are much better localized in space than massless photons [2]. The dissociation process of  $\text{H}_2^+$  we are studying here shows similar to the above-mentioned two-particle quantum correlations. They originate from a strong delocalization of an electron over two protons which intuitively should be localized on just one of the protons when they are separated by the distance  $R$  much larger than the atomic Bohr orbit.

In this paper we investigate theoretically an experimental scheme based on recent advances in the ultrashort laser technologies which allow one to shape laser pulses in femtosecond or even subfemtosecond (attosecond) timescales [12,13]. Thus, these technologies allow one to image the evolution in time of correlated electron-nuclear wave function. This can be achieved by initiating the dissociation process

using an ultrashort pump pulse and allowing the dissociating fragments to separate and be far apart. Next, this system can be probed via a photoionization process using a probe pulse having a well-defined phase relative to the pump pulse, and consequently in phase with the dissociating system. In general, the photoelectron spectra will exhibit a two-center interference, sometimes called a Fano interference since it was predicted by Cohen and Fano in 1967 [14]. Their calculations showed that when a molecule is photoionized via absorption of one photon the photoelectron spectra in diatomic molecules are modulated by an interference factor,

$$\bar{\chi} = 1 \pm \frac{\sin(|\vec{p}_e|R_{\text{eq}})}{|\vec{p}_e|R_{\text{eq}}}, \quad (1)$$

where  $\vec{p}_e$  is the electron momentum and  $R_{\text{eq}}$  is the equilibrium internuclear distance and the sign depends on the parity of the molecular electronic wave function; (+) for a gerade and (−) for an ungerade electronic state. We show that if the Fano interference is observed in dissociating diatomic molecule at large internuclear separation it may become an important tool for visualizing peculiarities of quantum mechanics related to entanglement and to the nonlocal character of the electron which (intuitively) should be localized on a single heavy (1836.15 times heavier than the electron) center, during the dissociation process, due to localization via Coulomb attractive force. Note that a quantum state describing a localized electron on a specific proton accompanying another distant proton would not lead to the two-center Fano interference in the photoelectron spectrum. This interference is a result of the unique gerade or ungerade symmetry of the electronic molecular wave function before the photoionization takes place. Since the molecular Hamiltonian has also this symmetry we conclude that the state before the turn-on of the probe pulse should preserve the symmetry of the dissociating state prepared by a pump pulse. In other words, the quantum dissociating state is not a simple product of the hydrogen and proton states but is a coherent superposition of the possible “simultaneous presence” of the electron on both well-separated protons.

\*S.Chelkowski@usherbrooke.ca

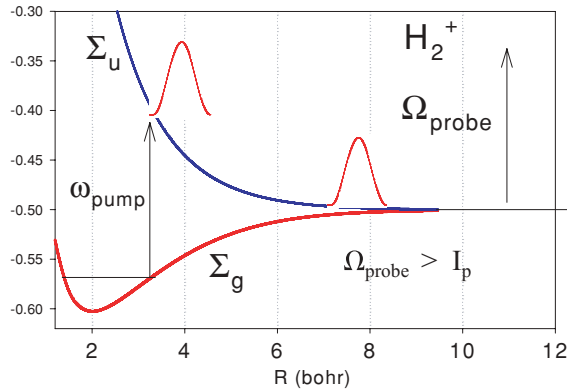


FIG. 1. (Color online) Illustration of the proposed pump-probe experimental scheme. Two lowest electronic surfaces  $\Sigma_g$  and  $\Sigma_u$  of  $\text{H}_2^+$  are shown. The pump pulse prepares the nuclear wave packet sliding on the upper ungerade surface  $\Sigma_u$ . After the turn-off of the pump pulse this wave packet evolves as free system until it is photoionized at large internuclear distance  $R$ .

More specifically, we consider a pump-probe excitation scheme [12,13] in which a pump laser pulse prepares a dissociating nuclear wave packet on an ungerade (repulsive) surface of a  $\text{H}_2^+$  molecule. Next (20–200 fs later, after the pump pulse is turned off), an ultraviolet [or extreme ultraviolet (XUV)] probe pulse ionizes this dissociating (H-atom + proton) state at large ( $R = 20\text{--}150$  bohr) internuclear distance, as illustrated in Fig. 1 and also described in [13]. We show that coincidence measurement of the electron and proton spectra reveal a very special, counterintuitive nature of the quantum dissociation process. It can be assumed that after the turn-off of the pump pulse the motion on the ungerade surface of  $\text{H}_2^+$  is adiabatic. Consequently, because of the antisymmetric (or symmetric, if dissociation occurs on a gerade electronic state) character of the electronic wave function the quantum state of the dissociating system is very distinct from a simple product of a state of a free proton and a free hydrogen atom [15]. Such a simple product occurs (e.g., in proton-hydrogen scattering). Thus quantum mechanics predicts that even at large internuclear distance the electron can be well localized in two places (i.e., it can form a hydrogen atom on two well-separated protons which seems counterintuitive). Note that in our scheme electron localization occurs due to the Coulomb attraction from two protons. Suppose that we have measured the hydrogen atom at the right-hand side along the laser polarization vector, as shown in Fig. 2. Already at relatively small internuclear distance  $R = 10$  bohr shown in Fig. 2 the electron is very well localized on each center. Thus, we infer (using the charge conservation principle) that the opposite detector (at left-hand side in Fig. 2) at the internuclear separation larger than  $R = 60$  bohr will measure with a certitude a proton. This situation resembles a variant of the EPR paradox based on the disintegrating system of the two-spin one-half particles, originating from their initial singlet state [16] in which by measuring a spin up by one detector we infer what was the spin projection measured by the opposite detector.

Suppose now that instead of measuring directly the H atom in the above experiment we use a probe UV pulse which

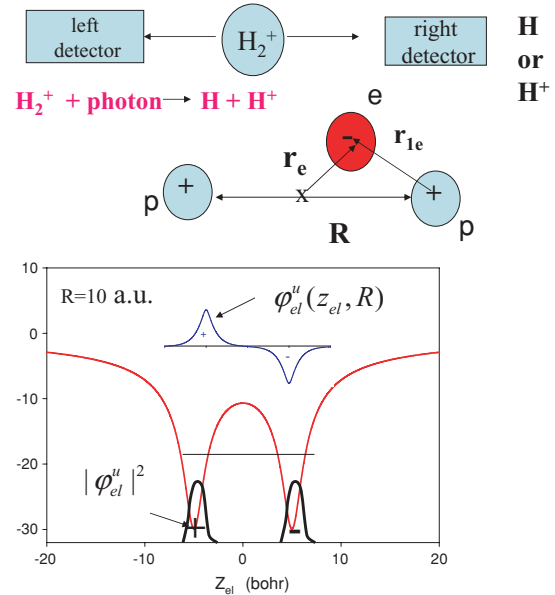


FIG. 2. (Color online) The upper part shows schematically the first stage of the proposed experimental scheme in the case when only the laser pump pulse is used. This pulse dissociates the  $\text{H}_2^+$  molecule. Two opposing detectors are measuring the H atom or the  $\text{H}^+$  ion. These measurements resemble the case of the EPR paradox in which the spin projections are measured in the disintegration of the two-spin one-half particles from the initial single-spin state. We also illustrate the definition of the Jacobi coordinates for the  $p$ - $p$ - $e$  system used in our calculations. The lower part shows the two-center Coulomb potential, the ungerade electronic wave function  $\varphi_{el}^u$  and the corresponding probability density as a function of the electron coordinate  $z_{el}$  at fixed internuclear distance  $R = 10$  bohr.

photoionizes the molecule and the two-center Fano interference pattern is observed in the photoionization signal. Simple perturbative calculations using a plane wave approximation for the final electrons state [14,17] predict that at fixed internuclear vector  $\vec{R}$  the molecular photoelectron signal is modulated via interference factors  $\sin^2(\vec{p}_e \cdot \vec{R}/2)$  or  $\cos^2(\vec{p}_e \cdot \vec{R}/2)$ . Just the fact that such an interference pattern is observed would mean that the electron is well localized simultaneously on system. This is a very unusual and counterintuitive situation since the tunneling time from one center to another is extremely large even at the relatively small internuclear separation  $R = 60$  bohr:  $t_{\text{tunnel}} = 2.4$  years [15]. Moreover, if we interpret the integral of  $e|\psi|^2$  over half-space as a charge present around a specific proton, one concludes that a fractional charge  $e/2$  is well localized around one center [18]. Thus, one may argue that the observation of the Fano two-center interference is a witness for the simultaneous presence of a charge  $e/2$  on each center. Clearly, this simple three-body system with the electron and two well-separated protons represents an interesting quantum mystery related to the formation of a hydrogen atom during the dissociation process and is certainly worth further experimental and theoretical investigation.

There exists already some experimental evidence for the existence of the Fano interferences originating from dissociating molecules at large internuclear separations: in the pump-probe experiment by Sanov *et al.* [19] negative iodine

$I_2^-$  ions were used in which similar to dissociating  $H_2^+$  electron delocalization occur when a following pump probe is used. The photoionization was initialized using a 780-nm laser that dissociated the  $I_2^-$  ions into  $I^- +$  neutral iodine atom I. After a variable time delay, a photoionizing probe removed the electron from the  $I_2^-$  ion. Next the asymmetry coefficient [19] was calculated from the photoelectron angular distributions. This coefficient oscillates as function of the time delay between the probe and pump pulses as expected from our calculations presented at the end of Sec. IV. This oscillation is due to the fact that as in this experimental scheme one cannot distinguish whether the photoelectron originates from the right or left iodine atom separated by an internuclear distance as large as 60 bohr.

In our theoretical description of the above-mentioned pump-probe scheme (dissociation followed by photoionization), we do not calculate the dynamics of the first step in which an ultrashort UV pump pulse photodissociates (via an absorption of one photon) the  $H_2^+$  molecule and it thus prepares a nuclear wave packet moving on the molecular ungerade surface. We assume that this wave packet has the Gaussian shape right after the pump pulse is turned off, centered at  $R = R_0 = 12$  bohr, at  $t = 0$ , and it next evolves as a free system (field-free) on the  $\Sigma_u$  surface until it reaches the internuclear distance  $R = 60\text{--}120$  bohr. Then an ultrashort UV pump laser pulse is turned on and it photoionizes this dissociating packet, at  $t = t_c$ , also via a one-photon process. The photoionization probability distributions of the momenta of the electron and the protons are calculated using first-order perturbation theory in three dimensions (3-D) (for both electron and nuclear degrees of freedom). A plane wave approximation is used for the final state of protons and a “modified-plane-wave” approximation for the electron (see next section for the details). Note that to the best of our knowledge, all theoretical work related to Fano interference has been so far done using frozen nuclei at fixed equilibrium internuclear distance  $|\vec{R}_{eq}|$ . We believe that our study is the first dynamical investigation of Fano interference in the photoelectron spectrum originating from dissociating molecules at large internuclear separations. It includes full 3-D electron-nuclear dynamics. Note that so far approaches based on solving the time-dependent Schrödinger equation for  $H_2^+$  are based on the models with reduced dimensionality [20,21].

## II. PERTURBATIVE CALCULATIONS OF DISSOCIATIVE IONIZATION

We use Jacobi coordinates for the electron and two protons (separated by a vector  $\vec{R}$ ) in which the electron position vector  $\vec{r}_e$  originates in the center of mass of two protons; see Fig. 2. In these coordinates, the Hamiltonian of  $H_2^+$  has the following form [22] (in atomic units,  $\hbar = m_e = e = 1$ ):

$$\hat{H}_0 = -\frac{1}{2m'_e} \Delta_{\vec{r}_e} - \frac{1}{2\mu} \Delta_{\vec{R}} + V_C(\vec{r}_e, \vec{R}), \quad (2)$$

where

$$m'_e = \frac{2m_p m_e}{2m_p + m_e}, \quad \mu = m_p/2$$

are the electron two-proton reduced mass and the proton-proton reduced mass, respectively,

$$V_C(\vec{r}_e, \vec{R}) = \frac{-1}{|\vec{r}_e - \vec{R}/2|} + \frac{-1}{|\vec{r}_e + \vec{R}/2|} + \frac{1}{|\vec{R}|} \quad (3)$$

is the total Coulomb interaction between protons and the electron, and  $m_e$  and  $m_p$  are the electron and proton masses. The total Hamiltonian is  $\hat{H} = \hat{H}_0 + \hat{V}_{int}$ , where

$$\hat{V}_{int} = -i \frac{\kappa}{m'_e c} \vec{A}(t) \cdot \vec{\nabla}_{\vec{r}_e}, \quad (4)$$

where

$$\kappa = 1 + \frac{m_e}{2m_p + m_e}.$$

$\hat{V}_{int}$  describes the interaction of  $H_2^+$  with a UV laser probe field via its vector potential. Since we use a weak intensity probe pulse and the pulse frequency is larger than the ionization potential of  $H_2^+$  we may use the perturbation theory for calculation of the photoionization probability of the dissociating wave packet (prepared by the pump pulse) using the transition amplitude:

$$A_{fi} = -i \int_{-\infty}^{\infty} dt \langle \psi_f | e^{i\hat{H}_0 t} \hat{V}_{int} e^{-i\hat{H}_0 t} | \psi_{in}(t) \rangle. \quad (5)$$

We first recall the result for fixed nuclei at  $\vec{R}$ . Using for the electron initial state,

$$\varphi_{el}^{g/u}(\vec{r}_e, \vec{R}) = \frac{1}{\sqrt{2}} [\psi_H(\vec{r}_e + \vec{R}/2) \pm \psi_H(\vec{r}_e - \vec{R}/2)], \quad (6)$$

where  $\psi_H$  is the hydrogen 1s wave function [sign ( $\pm$ ) is used for the electronic gerade on the ungerade state], and using the plane wave for the final electron state:

$$\psi_f = (2\pi)^{-3/2} \exp(i\vec{p}_e \cdot \vec{r}_e), \quad (7)$$

we get from Eq. (5) (just by choosing the integration coordinates local to each center) that

$$|A_{fi}^{fix}|^2 \sim [1 \pm \cos(\vec{p}_e \cdot \vec{R})] |A_H(\vec{p}_e)|^2, \quad (8)$$

where  $A_H(\vec{p}_e)$  is the atomic photoionization amplitude given in [17]. Thus, if ionization occurs from the ungerade surface the molecular ionization probability is modulated via a  $\sin^2(\vec{p}_e \cdot \vec{R}/2)$  factor. If the molecule is not initially aligned, and if protons momenta are not measured, we need to integrate over the direction of  $\vec{R}$  which leads to the  $\bar{\chi}$  factor given in Eq. (1). To include the nuclear motion in Eq. (5) we use the plane wave approximation for the final state for both the electron and for the relative motion of protons:

$$\psi_f = (2\pi)^{-3} \exp(i\vec{p}_N \cdot \vec{R}) \exp(i\vec{p}_e \cdot \vec{r}_e). \quad (9)$$

We will isolate from this expression the electronic atomic photoionization amplitude  $A_H(\vec{p}_e)$  in which we will use the exact expression for an atomic amplitude, that is, in which exact Coulomb wave for the individual center is included (but the influence of the neighboring center is neglected which is a reasonable approximation for the case of very large  $R$  we are interested in). This explains the term “modified-plane-wave” approximation used in the introduction. Regarding the plane wave approximation for the nuclei we think that

it is justified for photoionization occurring at very large internuclear distances. We are interested in  $R$ 's as large as  $R > 60$  bohr at which Coulomb repulsion should be negligible with respect to the kinetic energy of the the dissociating  $\text{H}_2^+$ , that is, when

$$\frac{p_0^2}{2\mu} \gg \frac{e^2}{R_0 + p_0 t_c / \mu}, \quad (10)$$

where  $R_0$  is the position of the the center of the dissociating wave packet with the momentum  $p_0$  at  $t = 0$  when the pump pulse is turned off and  $t_c$  is the time at which the amplitude of the probe pulse is at maximum. At this time the wave packet reaches the distance  $R_0 + p_0 t_c / \mu$ . These plane wave approximations allow us to get a simple analytic expression for the amplitude  $A_{fi}$ . Using the Coulomb waves in the final state leads one to much more complicated formulas involving some numerical integration.

As the initial state we take the Born-Oppenheimer solution (we consider an improvement to this approximation in the appendix) as a product of the ungerade electronic function (6) and the superposition of nuclear plane waves  $\exp(i\vec{p} \cdot \vec{R})$ :

$$\psi_{\text{in}}(\vec{r}_e, \vec{R}, R_0) = \varphi_{\text{el}}^u(\vec{r}_e, \vec{R}) \int d^3 p \varphi_N(\vec{p}, R_0) \exp(i\vec{p} \cdot \vec{R}), \quad (11)$$

where  $\varphi_N(\vec{p}, R_0)$  is the initial distribution of the momenta in the dissociating nuclear wave packet. It should be adjusted to the shape of the wave packet prepared by the pump pulse which we suppose is short (its duration is 5–20 fs). In calculation of the amplitude (5) we assume the free evolution of the  $\text{H}_2^+$  wave packet between the turn-off of the pump pulse at  $t = 0$  and the turn-on of the probe pulse. We derive next the analytic formula for photoionization valid for any shape of  $\varphi_N(\vec{p}, R_0)$ . Its specific shape will be chosen for illustrating graphically our results. In order to perform analytically the time integral in (5) we need a specific shape of the vector potential  $\vec{A}(t)$  of the laser field. We assume it has a Gaussian form:

$$\vec{A}(t) = \frac{\vec{e}_{\text{probe}}}{2} A_0 \exp\left[-\frac{(t - t_c)^2}{2\tau^2}\right] \exp(-i\Omega_{\text{probe}} t) + \text{c.c.}, \quad (12)$$

where  $A_0$ ,  $\vec{e}_{\text{probe}}$ ,  $\Omega_{\text{probe}}$ , and  $\tau$  are the UV probe pulse amplitude, polarization, central frequency, and duration. Pulse duration  $\tau$  is related to the commonly used FWHM duration via relation  $\tau_{\text{FWHM}} = 2\sqrt{\ln(2)}\tau$ . We recall that thus defined FWHM means full width at half-maximum of the laser intensity time profile, not the FWHM of the envelope of the laser field.  $t_c$  is the time at which the probe pulse has maximum and at the same time  $t_c$  is also a measure the time delay between the probe and the pump pulse since we have chosen  $t = 0$  as the time when the pump pulse is turned off and the center of the nuclear packet is at  $R = R_0$ .

After integrating the time  $t$  and the electronic coordinate  $\vec{r}_e$  in the formula (5), we get:

$$A_{fi} = N_1 A_H(\vec{p}_e) \int d^3 p a(\vec{p}) \int d^3 R \times \exp(i\vec{p} \cdot \vec{R} - i\vec{p}_N \cdot \vec{R}) (e^{i\vec{p}_e \cdot \vec{R}/2} - e^{-i\vec{p}_e \cdot \vec{R}/2}), \quad (13)$$

where

$$a(\vec{p}) = \exp[if(\vec{p})t_c - \tau^2 f(\vec{p})/2] \varphi_N(\vec{p}, R_0), \quad (14)$$

$$f(\vec{p}) = \frac{\vec{p}_e^2}{2m'_e} + \frac{\vec{p}_N^2}{2\mu} + I_p - \Omega_{\text{probe}} - \frac{\vec{p}^2}{2\mu}, \quad (15)$$

$$N_1 = \frac{\kappa A_0 \tau}{2\pi 2^{3/2} m'_e c},$$

$$A_H(\vec{p}_e) = A_{1s}(\vec{p}_e) = 2^{3/2} \frac{(\vec{e} \cdot \vec{p}_e)(1 - i\nu)}{\pi(1 + \vec{p}_e^2)^2} \times \exp[-2\nu \arctan(p_e)] N_v^*, \quad (16)$$

$$\nu = \frac{1}{p_e}, \quad N_v = \exp(\pi\nu/2)\Gamma(1 + i\nu).$$

Integration over the  $\vec{R}$  coordinate yields two Dirac delta functions for momentum conservation. Thus, we get for the dissociative-ionization amplitude,

$$A_{fi} = N_1 (2\pi)^3 A_H(\vec{p}_e) \int d^3 p a(\vec{p}) [\delta(\vec{p} - \vec{p}_N + \vec{p}_e/2) - \delta(\vec{p} - \vec{p}_N - \vec{p}_e/2)]. \quad (17)$$

Integration over the nuclear momenta  $\vec{p}$  yields the final probability amplitude for dissociative ionization,

$$A_{fi} = N_2 A_H(\vec{p}_e) [a(\vec{p}_-) - a(\vec{p}_+)], \quad (18)$$

where  $a(\vec{p})$  is defined in (14),

$$N_2 = (2\pi)^3 N_1 = \frac{\kappa A_0 (2\pi)^2 \tau}{2^{3/2} m'_e c},$$

and

$$\vec{p}_{\pm} = \vec{p}_N \pm \vec{p}_e/2. \quad (19)$$

The shifted momentum in the last equation is related to the recoil received by each proton from the electron: the final relative momentum is either  $\vec{p}_+$  or  $\vec{p}_-$ .

Equation (18) provides a general expression for the momenta distributions of protons and of the electron valid for any initial distribution of momenta  $\varphi_N(\vec{p}, R_0)$  of a dissociating wave packet. However, in order to investigate in detail Fano two-center interference effect we need to specify the initial momentum distribution in the wave packet prepared by the pump pulse. We suppose that the  $\text{H}_2^+$  molecule was initially in the vibrational  $v = 0$ ,  $J = 0$  of the gerade bound state, where  $J$  is the initial angular momentum quantum number of the molecule. Thus, the nuclear wave packet, after absorption of one photon, will be in the  $J = 1$  rotational state on the ungerade  $\Sigma_u$  surface of  $\text{H}_2^+$ . We assume that it has the form:

$$\varphi_N(\vec{p}, R_0) = C_N \frac{\cos \theta_p}{p} \exp\left(-\frac{\Delta R^2}{2}(p - p_0)^2\right) \times \exp[i(p_0 - p)R_0], \quad (20)$$

where  $\cos \theta_p = \vec{p} \cdot \vec{e}_{\text{pump}}/|\vec{p}|$  and  $\theta_p$  is the angle between the nuclear relative momentum  $\vec{p}$  and the pump pulse polarization.

The nuclear wave packet is at  $R = R_0$  at  $t = 0$ , the probe has maximum at  $t = t_c$ . This is a free Gaussian wave packet (in the radial variable  $p = |\vec{p}|$ ) sliding on the electronic surface  $\Sigma_u$  with the angular momentum  $J = 1$ . Its electronic wave function  $\varphi_{el}^u$  is given in Eq. (6). The central radial momentum of the wave packet is  $p_0$  and its spatial width is  $\Delta R$ . In order to study the two-center interference effect it is convenient to rewrite the probability of ionization in the following form (in this form the interference appears through the cross term  $C$ ):

$$|A_{fi}(\vec{p}_e, \vec{p}_N, \tau, \Delta R, t_c)|^2 = |A_H(\vec{p}_e)|^2 [ |a(\vec{p}_+)|^2 + |a(\vec{p}_-)|^2 + C(p_+, p_-, t_c) ], \quad (21)$$

where

$$|a(\vec{p})| = C_N \exp\left(-f^2(\vec{p}) \frac{\tau^2}{2} - \frac{\Delta R^2}{2}(p - p_0)\right) |\vec{p} \cdot \vec{e}| / |\vec{p}|^2, \quad (22)$$

$$C(p_+, p_-, t_c) = 2|a(\vec{p}_+)| |a(\vec{p}_-)| \cos[\Phi(t_c)], \quad (23)$$

$$\begin{aligned} \Phi(t_c, \vec{p}_e, \vec{p}_N) &= (|\vec{p}_+| - |\vec{p}_-|)R_0 + [f(\vec{p}_-) - f(\vec{p}_+)]t_c \\ &= (|\vec{p}_+| - |\vec{p}_-|)R_0 + \frac{|\vec{p}_+|^2 - |\vec{p}_-|^2}{2\mu} t_c. \end{aligned} \quad (24)$$

After the use of Eq. (19), the phase  $\Phi$  becomes

$$\Phi(t_c, \vec{p}_e, \vec{p}_N) = (|\vec{p}_+| - |\vec{p}_-|) R_0 + \vec{p}_e \cdot \frac{\vec{p}_N}{\mu} t_c. \quad (25)$$

This is an important result since after comparing Eq. (25) with the phase corresponding to static result Eq. (8) we conclude that by measuring the relative nuclear momentum  $p_N$  and the delay time  $t_c$  we are fixing the increment of the internuclear separation  $\vec{R}$  during the time interval  $t_c$  (i.e., this increment is simply):  $\vec{v}_N t_c$  where  $\vec{v}_N = \vec{p}_N / \mu$  is the relative velocity of protons. We can simplify more Eq. (25) in the case of the nuclear momentum larger than the electron momentum (i.e., if the inequality  $p_e \ll p_N$  holds we get):

$$\begin{aligned} |\vec{p}_\pm| &= \sqrt{p_N^2 \pm \vec{p}_e \cdot \vec{p}_N + p_e^2/4} \simeq p_N \pm \vec{p}_e \cdot \frac{\vec{p}_N}{2p_N} \\ &= p_N \pm p_e \cos(\theta_{pe})/2. \end{aligned} \quad (26)$$

Thus, the phase (25) on which the interference relies simplifies:

$$\Phi(t_c, \vec{p}_N) \simeq \vec{p}_e \cdot \vec{R}_N(t_c, \vec{p}_N), \quad (27)$$

where

$$\vec{R}_N(t_c, \vec{p}_N) \simeq R_0 \frac{\vec{p}_N}{|\vec{p}_N|} + \frac{\vec{p}_N t_c}{\mu}. \quad (28)$$

We will also use later the absolute value of the vector  $\vec{R}_N$ :

$$R_N(t_c, p_N) = |\vec{R}_N(t_c, \vec{p}_N)| \simeq R_0 + \frac{p_N t_c}{\mu}. \quad (29)$$

Clearly, we see from the last equations that, as in the case of static result (8) the interference term  $C(p_+, p_-, t_c)$  is modulated via the term  $\cos[R_N(t_c, p_N) p_e \cos(\theta_{ep})]$ , where  $\theta_{ep}$  is the angle between the electron momentum and relative nuclear momentum  $\vec{p}_N$ . This relation can be used for imaging the nuclear motion as suggested in [13]: If we measure the

ionization signal for a series of time delays  $t_c$  and follow the change of a specific minimum in the spectrum, we can thus deduce the molecular trajectory from the relation  $2n\pi/p_e \cos(\theta_{ep})$ , where  $n$  is an integer corresponding to a specific minimum. If, furthermore, the width of the momentum distribution  $\frac{1}{\Delta R}$  is sufficiently large compared to the electron momentum  $p_e$  (i.e.,  $p_e < \frac{1}{\Delta R}$ ), we may expect that the following approximations are valid for  $p_N$  values close to the central value  $p_0$  of the momentum distributions defined via (20):

$$|a(\vec{p}_-)| \simeq |a(\vec{p}_+)| \simeq |a(\vec{p}_N)|, \quad (30)$$

we get

$$\begin{aligned} |A_{fi}|^2 &\sim |A_H(\vec{p}_e)|^2 \sin^2\left(\vec{p}_e \cdot \frac{\vec{p}_N}{|\vec{p}_N|} R_N(t_c, |\vec{p}_N|)/2\right) \\ &\times \left[\frac{\vec{p}_N \cdot \vec{e}_{\text{pump}}}{p_N^2}\right]^2 \end{aligned} \quad (31)$$

or

$$|A_{fi}|^2 \sim \cos^2(\theta_e) \sin^2[p_e \cos \theta_{pe} R_N(t_c, |\vec{p}_N|)/2] \cos^2(\theta_p), \quad (32)$$

where  $\theta_e$  is the angle between the electron momentum and the probe pulse polarization vector  $\vec{e}_{\text{probe}}$ , and  $\theta_p$  is the angle between the  $\vec{p}_N$  vector and the pump polarization  $\vec{e}_{\text{pump}}$ . Assuming that initially  $\text{H}_2^+$  was at rest with the initial momentum of  $\text{H}_2^+$  center of mass  $\vec{P}_{\text{c.m.}}$  is zero, we have the following relations between the measured final momenta of the two protons  $\vec{p}_1, \vec{p}_2$ , and of the electron momentum  $\vec{p}_e$  and the relative nuclear momentum  $\vec{p}_N$ :

$$\vec{p}_1 + \vec{p}_2 + \vec{p}_e = \vec{P}_{\text{c.m.}} = 0 \quad \vec{p}_N = \frac{1}{2}(\vec{p}_1 - \vec{p}_2). \quad (33)$$

Consequently, if the initial molecular temperature is zero it will be sufficient to measure the electron momentum and the momentum of one proton  $\vec{p}_1$  in order to determine the  $\vec{p}_N$  vector on which the interference relies. Thus, the vectors present in (21) formulas become:

$$\vec{p}_N = \vec{p}_1 + \vec{p}_e/2, \quad \vec{p}_+ = \vec{p}_1 + \vec{p}_e, \quad \vec{p}_- = \vec{p}_1. \quad (34)$$

In the case of nonzero temperature of initial  $\text{H}_2^+$  translational motion one should either average our formula over thermal momenta of  $\text{H}_2^+$  or measure in coincidence the momenta of all three fragments resulting from the photoionization of dissociating  $\text{H}_2^+$  in order to avoid possible washing out of the interference term.

Summarizing our most important result is that the Fano two-center interference shows up in the cross term  $C(p_+, p_-, t_c)$  in Eq. (23) via

$$\cos[\vec{p}_e \cdot \vec{R}_N(t_c, \vec{p}_N)], \quad (35)$$

where  $\vec{R}_N(t_c, \vec{p}_N)$  is given in Eq. (28). Note that the calculations in which  $\vec{R}$  is fixed lead instead to the very similar interference term  $\cos(\vec{p}_e \cdot \vec{R})$  in Eq. (8). Thus, the effect of nuclear motion consists of replacing  $R$  by  $\vec{R}_N(t_c, \vec{p}_N)$  which is a simple linear function of the final relative momentum of outgoing protons  $\vec{p}_N$  and of the time delay  $t_c$ . A convenient way to analyze this interference in the case of  $\vec{p}_N$  fixed and parallel to the probe polarization  $\vec{e}_{\text{probe}}$  [note then  $\theta_e = \theta_{pe}$  which simplifies

significantly Eq. (32) is to expand the angular distributions described by (32) in Legendre polynomials  $P_l(\cos\theta_e)$ :

$$\begin{aligned} |A_{fi}|^2 &\sim \cos^2\theta_e [1 - \cos(p_e R \cos\theta_e)] \\ &= \cos^2\theta_e \left[ 1 - \sum_{l=0, l-\text{even}}^{\infty} (2l+1) j_l(p_e R(t_c)) P_l(\cos\theta_e) i^l \right], \end{aligned} \quad (36)$$

$$|A_{fi}|^2 \sim \beta_0(t_c) + \beta_2(t_c) P_2(\cos\theta_e) + \beta_4(t_c) P_4(\cos\theta_e), \quad \text{where} \quad (37)$$

$$\beta_0 = \frac{1}{3} [1 - j_0 + 2j_2] \simeq \frac{1}{3} \left[ 1 - 3 \frac{\sin[p_e R_N(t_c, p_N)]}{p_e R_N(t_c, p_N)} \right] \quad \text{for } p_e R(t_c) \gg 1, \quad (38)$$

$$\begin{aligned} \beta_2 &= \frac{1}{3} \left[ 2 - j_0 + \frac{55}{7} j_2 - \frac{36}{7} j_4 \right] \\ &\simeq \frac{1}{3} \left[ 2 - \frac{92}{7} \frac{\sin[p_e R_N(t_c, p_N)]}{p_e R_N(t_c, p_N)} \right] \quad \text{for } p_e R(t_c) \gg 1, \end{aligned} \quad (39)$$

$$\beta_4 = \frac{30}{11} j_6 - \frac{351}{77} j_4 \simeq \frac{51}{7} \frac{\sin[p_e R_N(t_c, p_N)]}{p_e R_N(t_c, p_N)} \quad \text{for } p_e R(t_c) \gg 1. \quad (40)$$

We see clearly that the expansion of angular distributions in Legendre polynomials reveals the Fano interference as a function of the pump-probe time delay  $t_c$  in a very neat way. An analysis of experimental data related to the Fano interference using such an expansion was recently performed, for example, in [19]. More specifically, in [19] a pump-probe experiment was reported in which a pump pulse photodissociates a  $\text{I}_2^-$  molecule and the probe photoionizes the dissociating molecule. The  $\beta_2(t_{\text{delay}})$  coefficient calculated from the experimental photoelectron angular distribution shows the modulation similar to oscillations expected from our Eq. (39). These experimental oscillations in  $\beta_2(t_{\text{delay}})$  do not survive for the time delays larger than a few picoseconds. We suggest that this may be related to the constant term present in Eq. (39) which shows in the experiment as background or they disappear due to averaging over nuclear momenta which becomes more significant at larger internuclear separations. Note that the higher  $\beta_4(t_c)$  coefficient does not contain any constant term and thus may yield a better contrast allowing the Fano interference to survive for larger time delays.

### III. SOME SPECIFIC EXAMPLES OF THE PROPOSED PUMP-PROBE EXPERIMENTS

The interference expected from the theory presented in the previous section will show up most clearly when the proton and the electron momenta are measured in coincidence. Using

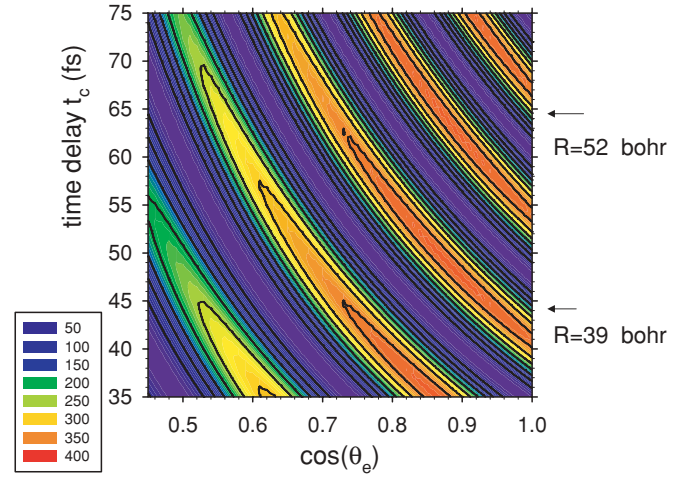


FIG. 3. (Color online) Ionization probability (multiplied by  $10^4$ ) calculated using Eqs. (21)–(24) for the case when the polarizations of the pump and probe pulses are parallel and the nuclear relative momentum  $\vec{p}_N$  is also parallel to both polarizations. We used  $\lambda_{\text{probe}} = 60$  nm,  $p_N = p_0 = 14.8$  a.u.,  $p_e = 0.72$  a.u.,  $\Delta R = 3.0$  bohr,  $R_0 = 12.0$  bohr, and the pump pulse duration  $\tau_{\text{FWHM}} = 2.4$  fs.

our exact expressions (21) for probabilities as a function of the momenta of three outgoing fragments, we calculate the probabilities of ionization by the probe pulse for three selected geometries and plot the results in Figs. 3–6. Note that we do not use in Figs. 3–5 the approximations suggested in formulas (26) and (30). The probabilities are shown as functions of the time delay  $t_c$  between the pump and the probe pulse. We plot in Fig. 3 the angular distributions of the electron

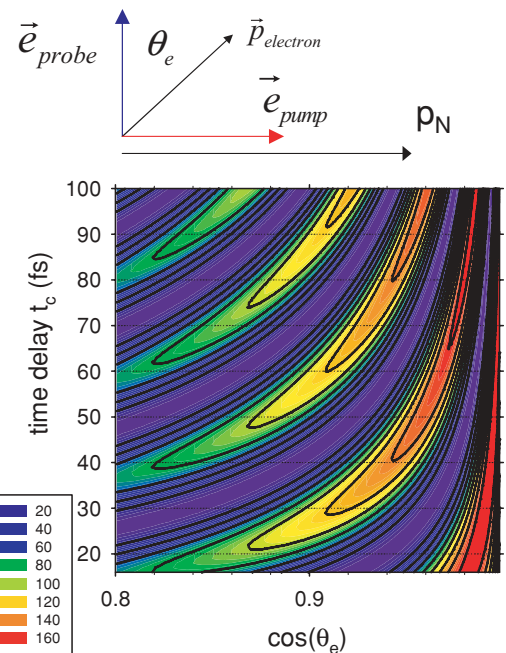


FIG. 4. (Color online) Same as in Fig. 3, but for the case when the polarizations of the pump and probe pulses are perpendicular and the nuclear relative momentum  $\vec{p}_N$  is also parallel to the polarization of the pump pulse as shown in the upper part of the figure.

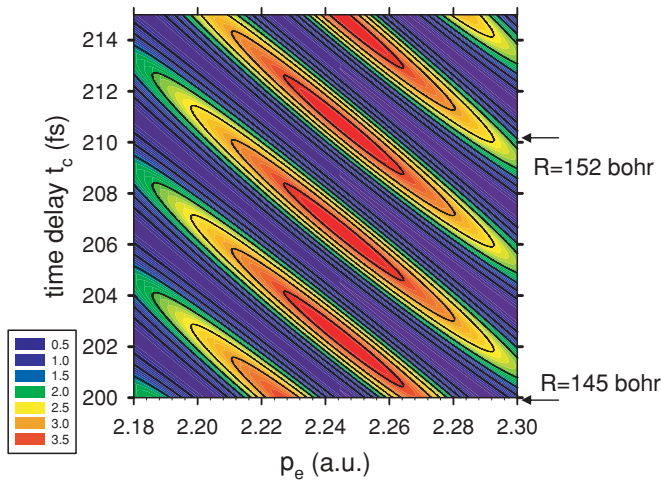


FIG. 5. (Color online) Same as in Fig. 3, but for the shorter pump wavelength  $\lambda_{\text{probe}} = 15$  nm, shorter pulse duration  $\tau_{\text{FWHM}} = 0.24$  fs and smaller width of the wave packet  $\Delta R = 1.0$  bohr. Note that now the electron angle  $\theta_e$  is fixed and equal to zero. The ionization probability is plotted now as a function of the electron momentum  $p_e$ .

in the parallel case (i.e., all three vectors  $\vec{e}_{\text{pump}}$ ,  $\vec{e}_{\text{probe}}$ , and  $\vec{p}_N$  are parallel and the momenta  $p_e$  and  $p_N$  are fixed at their values corresponding to the maximum probability. In Fig. 4, the perpendicular geometry is used (i.e., we choose the case of the pump laser polarization  $\vec{e}_{\text{pump}}$  perpendicular to polarization of the probe pulse  $\vec{e}_{\text{probe}}$ ). In Fig. 6 again the geometry is parallel as in Fig. 5 but instead of angular distributions we plot there the electron spectra for the electron flying along the polarization vectors. All three graphs show strong interference structures as a function of the time delay, as expected from the approximate factor  $\sin^2(\vec{p}_e \cdot \frac{\vec{p}_N}{|\vec{p}_N|} R_N(t_c, p_N)/2)$ . Note that we show in Figs. 3 and 5 the positions of the center of the wave

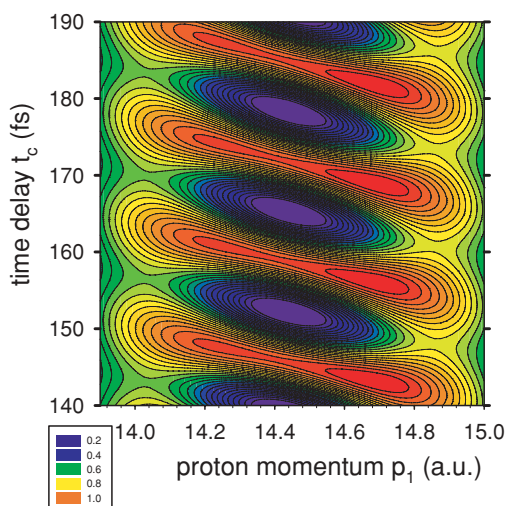


FIG. 6. (Color online) Same as in Fig. 3, but now the ionization probability is plotted now as function of the proton momentum  $p_1$  at fixed electron angle  $\theta_e = 0$ .

packet corresponding to certain time delays calculated using Eq. (29). Similar interference structures appear in the proton spectra displayed in Fig. 6 in which we are showing spectra as a function of the single-proton momentum  $p_1 = |\vec{p}_1|$  with fixed electron momentum  $p_e = 0.72$  a.u.. The  $\vec{p}_N$  vector is calculated using Eq. (34).

Note that in order to observe experimentally a sharp interference structure as plotted in Figs. 3–5 the momenta of the electron and of at least one proton should be measured in coincidence. Such measurements are possible due to the recently developed cold target recoil ion momentum spectroscopy (COLTRIMS) technique [23].

#### IV. CONCLUDING REMARKS

Summarizing, we have investigated a laser pump-probe scheme in which the measurement of the momenta distributions of the photoelectron allow one to determine the nuclear trajectory  $R(t)$  which simply plays a role of a slit separation in this double-slit-like experiment in which the molecule is “illuminated from within” [13]. Thus the probe pulse prepares the electron source whose de Broglie wave creates interference structure. The observed modulation as a function of time delay, due to the change of the slit separation becomes a witness of the simultaneous presence of the electron on each proton. In other words, when the internuclear distance  $R$  is much larger than the bohr orbit it would be natural to expect a localized electron on one heavy proton but such a localization would prevent the interference seen in the photoionization signal.

We have proposed a method (based on two-center Fano interference) for observing a very peculiar time-dependent quantum state which is an adiabatically stretched  $\text{H}_2^+$  molecule. This symmetry preserving stretching leads to the presence of a single electron on the two remote protons, well localized on each of them. In any local classical theory such an unusual presence would be impossible. This suggests that when the Fano interference is observed this might be interpreted as a witness to the nonlocal character of quantum mechanics. Moreover, we believe that this dissociating state is a very special kind of an entangled state of an electron and two protons. By definition, given in the second paragraph in Ref. [7], entanglement means nonfactorization of a two-particle wave function. First, in any breakup process [7], this nonfactorization originates from the mere fact that the wave function of interacting particles is a product of a function depending on the relative coordinate times the center-of-mass wave function; see Eq. (26) in [7]. Thus, the dissociating particles  $|\text{H}\rangle$  and  $|\text{H}^+\rangle$  are entangled before they are photoionized. The antisymmetry of the electron wave function probably leads to more nonfactorization in this specific system in which a single electron is shared equally by two remote protons and thus additional entanglement may appear in our three-body quantum system [24]. We wish to investigate this issue in more detail in future work.

Another unusual feature of the proposed experimental scheme in this paper is the fact that it allows one to measure, in a sense, the sign of the spatial wave function; more specifically, the measurement we propose detects (in the case

of an ungerade initial state) the fact that the sign of the electronic wave function on one center is minus and on another remote center is plus. Namely, at large internuclear distance the electronic wave function is given:

$$\varphi_{\text{el}}^{g/u} = \frac{1}{\sqrt{2}}[\psi_H(\vec{r}_e + \vec{R}/2) \pm \psi_H(\vec{r}_e - \vec{R}/2)].$$

Thus, the probability density distribution  $|\varphi_{\text{el}}^{g/u}(z)|^2$  is identical for both parities at very large  $R$  values (see Fig. 2). Nevertheless, measuring the photoelectron signal allows one to distinguish between the gerade and ungerade case since the photoionization probability at fixed internuclear distance  $R$  is proportional to  $\cos^2(\vec{p}_e \cdot \vec{R}/2)$  in the case of dissociation occurring on the gerade electronic state whereas it is proportional to  $\sin^2(\vec{p}_e \cdot \vec{R}/2)$  in the ungerade case. This sensitivity of the photoelectron spectra to parity (gerade or ungerade) is very specific to this simple dissociation process and because of this feature this experimental scheme is very distinct from the electron two-slit diffraction.

Another method for the observation of the two-center interference was proposed in [15]. This method uses the probe pulse which does not ionize the dissociating molecule but is based on elastic (Thomson) photon scattering from the two centers in the dissociating  $\text{H}_2^+$ . Thus, this method, which resembles the double-slit experiment for photons, allows one to probe the entangled state in dissociating  $\text{H}_2^+$  on the internuclear distance larger than the method discussed in our paper since the wavelength 800-nm laser is much larger than the de Broglie wavelength used in our scheme. This method, as ours, shows the delocalization of the electron on two remote centers since both the Thomson scattering or photoionization (in the case of our method) rely on the presence of the electron on each center (i.e., neither Thomson scattering nor photoionization can occur simply on bare proton. This fact distinguishes both schemes (ours and that proposed in [15]) from a simple double-slit quantum effect.

#### ACKNOWLEDGMENTS

We gratefully acknowledge stimulating discussions with C. L. Cocke, M. Vrakking, A. Sanov, and C.-D. Lin.

#### APPENDIX: BEYOND THE BORN-OPPENHEIMER APPROXIMATION IN THE INITIAL STATE

The Jacobi coordinates  $\vec{r}_e, \vec{R}$  used in Sec. II are not convenient at large internuclear distances  $R$  since the wave functions  $\exp(i\vec{p} \cdot \vec{R})\varphi_H^u(\vec{r}_e \pm \vec{R})$  used in Eq. (11) are not the exact eigenstates of the molecular Hamiltonian even if one neglects the Coulomb repulsion and the attraction from the remote bare proton. These states are the approximate eigenstates of  $\hat{H}_0$ , within the Born-Oppenheimer approximation. Note that when a proton and a hydrogen atom are very far apart the exact eigenstates of  $\hat{H}_0$  are simply a product of two plane waves for a free proton motion—free motion of the center of mass of a hydrogen atom multiplied by the electronic wave function describing the  $1s$  electronic state of the hydrogen atom. Thus, when the proton and the hydrogen atom are far apart and they

move with relative momentum  $\vec{p}$  it is convenient to rewrite the Hamiltonian  $\hat{H}_0$  using different Jacobi coordinates from that used in Sec. II. Namely, instead of using the internuclear vector  $\vec{R}$  and the electron coordinate  $\vec{r}_e$  we now use the vectors,

$$\begin{aligned} \vec{R}_1 &= \vec{R} + \alpha\vec{r}_{1e}, \quad \text{where} \quad \vec{r}_{1e} = \vec{r}_e - \vec{R}/2 \quad \text{and} \\ \alpha &= \frac{m_e}{m_e + m_p}. \end{aligned} \quad (\text{A1})$$

$\vec{R}_1$  is the relative vector between the center of mass of a hydrogen atom and the neighboring proton,  $\vec{r}_{1e}$  is the relative vector between the proton and the electron. In these coordinates, the Hamiltonian of  $\text{H}_2^+$  has the following form (in atomic units,  $\hbar = m_e = e = 1$ ):

$$\begin{aligned} \hat{H}_0 &= -\frac{1}{2m_e''}\Delta_{\vec{r}_{1e}} - \frac{1}{2\mu''}\Delta_{\vec{R}_1} - \frac{1}{|\vec{r}_{1e}|} + V_2(\vec{r}_e, \vec{R}), \\ \text{where} \quad V_2 &= -\frac{1}{|\vec{r}_e + \vec{R}/2|} + \frac{1}{R}, \end{aligned} \quad (\text{A2})$$

where

$$\mu'' = \frac{m_p(m_p + m_e)}{2m_p + m_e}, \quad m_e'' = \frac{m_p m_e}{m_p + m_e}, \quad (\text{A3})$$

and  $m_e''$  is simply the reduced mass of the electron in the hydrogen atom. Note that as in Jacobi coordinates used in Sec. II there is no cross gradient term with coupling nuclear and electronic variables. We easily find the exact eigenstates of a dissociating wave packet with the relative momentum  $\vec{p}$ , in these new Jacobi coordinates, in the limit of a very large internuclear distance when the potential  $V_2(\vec{r}_e, \vec{R})$  can be neglected. This exact asymptotic eigenstate has the following form:

$$\begin{aligned} \psi_{\text{in}}^{\text{asym}}(\vec{r}_e, \vec{R}, \vec{p}) &= \exp(i\vec{p} \cdot \vec{R}_1)\psi_H(\vec{r}_{1e}) \\ &= \exp[i\vec{p} \cdot (\vec{R} + \alpha\vec{r}_{1e})]\psi_H(\vec{r}_e - \vec{R}/2), \end{aligned} \quad (\text{A4})$$

where  $\vec{p}$  is the momentum of the relative motion between the hydrogen atom and the remote proton. Note that in contrast to the previously used eigenstate (11) the above state does not have the inversion symmetry with respect to the inversion  $\vec{r}_e \rightarrow -\vec{r}_e$ . Since we expect that the initial state should have such an inversion symmetry (as being prepared via one-photon excitation of the gerade electronic state of a  $\text{H}_2^+$  molecule), we construct the ungerade initial state in the following way:

$$\begin{aligned} \psi_{\text{in}} &= \frac{1}{\sqrt{2}} \int d^3 p \varphi_N(\vec{p}, R_0) [\psi_{\text{in}}^{\text{asym}}(-\vec{r}_e, \vec{R}, \vec{p}) \\ &\quad - \psi_{\text{in}}^{\text{asym}}(\vec{r}_e, \vec{R}, \vec{p})]. \end{aligned} \quad (\text{A5})$$

Clearly, for each fixed  $\vec{p}$  this is an entangled state of the two particles: a free proton and a free hydrogen atom. We rewrite the interaction potential (4) in a slightly different form:

$$\begin{aligned} \hat{V}_{\text{int}} &= -i\vec{A}(t) \cdot \left( \frac{1}{m_e} \nabla_{\vec{r}_e} - i \frac{1}{m_p} \nabla_{\vec{r}_{1p}} - i \frac{1}{m_p} \nabla_{\vec{r}_{2p}} \right) \\ &= -i \frac{1}{m_e'' c} \vec{A}(t) \cdot \nabla_{\vec{r}_{1e}} - i \frac{1}{m_p} \vec{A}(t) \cdot \nabla_{\vec{r}_{2p}}. \end{aligned} \quad (\text{A6})$$

Note that we keep here the complete interaction of the laser field  $\vec{A}(t)$  with three charges whereas in the previous Jacobi coordinates (4) the interaction term with coupling to the system center of mass was not included. In the last term in the above formula we have merged together the interaction of the electron with the proton which binds the electron. The last term in Eq. (A6) will be neglected in the matrix element (5) since it describes the interaction of the bare proton in the case when we evaluate the term containing  $\psi_H(\vec{r}_{1e})$ , and vice versa for the term with  $\psi_H(\vec{r}_{2e})$ . Inserting this new initial state (A5) into Eq. (5) we get

$$\tilde{A}_{fi} = \tilde{N}_2[A_H(\vec{p}_e + \alpha\vec{p}_-)\tilde{a}(\vec{p}_-) - A_H(\vec{p}_e - \alpha\vec{p}_+)\tilde{a}(\vec{p}_+)], \quad (\text{A7})$$

where

$$\tilde{a}(\vec{p}) = \exp[i\tilde{f}(\vec{p})t_c - \tau^2\tilde{f}(\vec{p})/2]\varphi_N(\vec{p}, R_0), \quad (\text{A8})$$

and

$$\begin{aligned} \tilde{f}(\vec{p}) &= \frac{\vec{p}_e^2}{2m'_e} + \frac{\vec{p}_N^2}{2\mu} + I_p - \Omega_{\text{probe}} - \frac{\vec{p}^2}{2\mu''}, \\ \tilde{N}_2 &= (2\pi)^2 \frac{A_0\tau}{2^{3/2}m'_e c}, \end{aligned} \quad (\text{A9})$$

We note that using exact non-Born-Oppenheimer asymptotic (for large  $R$ ) states leads to the two following modifications in the transition amplitude as compared with (18). First, the atomic transition amplitude does not factorize; second, the function  $f(\vec{p})$  contains different reduced mass  $\mu''$ . The first modification has a simple interpretation: since the nuclei move in the opposite direction the relative electron momentum is different on each center (proton). Since the atomic amplitude  $A_H$  is now different at each center

previous Eqs. (21)–(23) will be modified in the following way:

$$\begin{aligned} &|\tilde{A}_{fi}(\vec{p}_e, \vec{p}_N, \tau, \Delta R, t_c)|^2 \\ &= |A_H(\vec{p}_e + \alpha\vec{p}_-)|^2 |\tilde{a}(\vec{p}_-)|^2 + |A_H(\vec{p}_e - \alpha\vec{p}_+)|^2 \\ &\quad \times |\tilde{a}(\vec{p}_+)|^2 + \tilde{C}(p_+, p_-, t_c) \end{aligned} \quad (\text{A10})$$

where

$$\begin{aligned} \tilde{C}(p_+, p_-, t_c) &= 2|a(\vec{p}_+)||a(\vec{p}_-)||A_H(\vec{p}_e + \alpha\vec{p}_-)| \\ &\quad \times A_H(\vec{p}_e - \alpha\vec{p}_+)|\cos[\tilde{\Phi}(t_c)], \end{aligned} \quad (\text{A11})$$

$$\begin{aligned} \tilde{\Phi}(t_c, \vec{p}_e, \vec{p}_N) &= (|\vec{p}_+| - |\vec{p}_-|) R_0 + \varphi_H(\vec{p}_e + \alpha\vec{p}_-) \\ &\quad - \varphi_H(\vec{p}_e - \alpha\vec{p}_+) + \vec{p}_e \cdot \frac{\vec{p}_N}{\mu''} t_c, \end{aligned} \quad (\text{A12})$$

where the phase  $\varphi_H(\vec{p})$  is simply the phase of the atomic amplitude  $A_H$  defined in Eq. (16), that is,

$$A_H(\vec{p}) = |A_H(\vec{p})| \exp[i\varphi_H(\vec{p})]. \quad (\text{A13})$$

We conclude that the Fano interference will be similar when the non-Born-Oppenheimer correction is included. The only change in the time-delay dependent part is a replacement of the reduced mass  $\mu$  by the mass  $\mu''$ . Another change, due to the shift of the argument in the  $A_H(\vec{p})$  function modifies only the term which does not depend on the time delay  $t_c$ . Moreover, the modifications discussed in this section will be negligible for the cases studied in Sec. III where the values of the electron and nuclear momenta are  $p_e = 0.72$ ,  $p_N = 14.8$  a.u., respectively, and  $\alpha = 1/1836$  is indeed small. Thus, we do not expect that the shifts in a slowly varying function  $A_H(\vec{p})$  will modify significantly the predictions relative to our “dynamic” Fano interference factor (23) and illustrated in previous sections in Figs. 3–6.

- 
- [1] A. Einstein, B. Podolsky, and N. Rosen, *Phys. Rev.* **47**, 777 (1935).  
[2] M. D. Reid, P. D. Drummond, W. P. Bowen, E. G. Cavalcanti, P. K. Lam, H. A. Bachor, U. L. Andersen, and G. Leuchs, *J. Mod. Phys.* **81**, 1727 (2009).  
[3] A. Ekert, *Phys. World* **22**(9), 29 (2009).  
[4] M. Aspelmeyer and A. Zeilinger, *Phys. World* **21**(7), 22 (2008).  
[5] J. Dunningham and V. Vedral, *Phys. Rev. Lett.* **99**, 180404 (2007).  
[6] M. V. Fedorov, M. A. Efremov, P. A. Volkov, and J. H. Eberly, *J. Phys. B* **39**, S467 (2006).  
[7] M. V. Fedorov, M. A. Efremov, A. E. Kazakov, K. W. Chan, C. K. Law, and J. H. Eberly, *Phys. Rev. A* **69**, 052117 (2004).  
[8] E. S. Fry, T. Walther, and S. Li, *Phys. Rev. A* **52**, 4381 (1995).  
[9] C. Gneiting and K. Hornberger, *Phys. Rev. Lett.* **101**, 260503 (2008).  
[10] T. Opatrny and G. Kurizki, *Phys. Rev. Lett.* **86**, 3180 (2001).  
[11] C. M. Savage and K. V. Kheruntsyan, *Phys. Rev. Lett.* **99**, 220404 (2007).  
[12] F. Krausz and M. Ivanov, *Rev. Mod. Phys.* **81**, 163 (2009).  
[13] M. Vrakking, *Physics* **2**, 72 (2009).  
[14] H. D. Cohen and U. Fano, *Phys. Rev.* **150**, 30 (1966).  
[15] V. P. Bykov and E. Nahvifard, *Las. Phys.* **13**(5), 501 (2003).  
[16] J. J. Sakurai, *Modern Quantum Mechanics*, Section 3.9 (The Benjamin/Cummings Publishing Company, Menlo Park, 1985).  
[17] G. L. Yudin, S. Chelkowski, and A. D. Bandrauk, *J. Phys. B* **39**, L17 (2006).  
[18] V. P. Bykov, *Physics-Uspekhi* **49**(9), 979 (2006).  
[19] R. Mabbs, K. Pichugin, and A. Sanov, *J. Chem. Phys.* **123**, 054329 (2005); **122**, 174305 (2005).  
[20] A. D. Bandrauk, S. Chelkowski, P. B. Corkum, J. Manz, and G. L. Yudin, *J. Phys. B* **42**, 134001 (2009).  
[21] A. D. Bandrauk and S. Chelkowski, *Phys. Rev. Lett.* **87**, 273004 (2001).  
[22] J. R. Hiskes, *Phys. Rev.* **122**, 1207 (1961).  
[23] R. Dörner, V. Mergel, O. Jagutzki, L. Spielberger, J. Ulrich, R. Moshhammer, and H. Schmidt-Böcking, *Phys. Rep.* **330**, 95 (2000).  
[24] S. Chelkowski and A. D. Bandrauk, e-print [arXiv:1001.3837](https://arxiv.org/abs/1001.3837) [quant-ph] (2010).